Endothelial Monocyte-Activating Polypeptide-II Induces BNIP3-Mediated Mitophagy to Enhance Temozolomide Cytotoxicity of Glioma Stem Cells via Down-Regulating MiR-24-3p

Jian Zhang [1,2], Libo Liu [3,4], Yixue Xue [3,4], Yawen Ma [1,2], Xiaobai Liu [1,2], Zhen Li [1,2], Zhiqing Li [3,4] and Yunhui Liu [1,2]*

[1] Department of Neurosurgery, Shengjing Hospital of China Medical University, Shenyang, China, [2] Liaoning Research Center for Translational Medicine in Nervous System Disease, Shenyang, China, [3] Department of Neurobiology, College of Basic Medicine, China Medical University, Shenyang, China, [4] Key Laboratory of Cell Biology, Ministry of Public Health of China, and Key Laboratory of Medical Cell Biology, Ministry of Education of China, Shenyang, China

Preliminary studies have shown that endothelial-monocyte-activating polypeptide-II (EMAP-II) and temozolomide (TMZ) alone can exert cytotoxic effects on glioma cells. This study explored whether EMAP-II can enhance the cytotoxic effects of TMZ on glioma stem cells (GSCs) and the possible mechanisms associated with Bcl-2/adenovirus E1B 19 kDa protein-interacting protein 3 (BNIP3)-mediated mitophagy facilitated by miR-24-3p regulation. The combination of TMZ and EMAP-II significantly inhibited GSCs viability, migration, and invasion, resulting in upregulation of the autophagy biomarker microtubule-associated protein one light chain 3 (LC3)-II/I but down-regulation of the proteins P62, TOMM 20 and CYPD, changes indicative of the occurrence of mitophagy. BNIP3 expression increased significantly in GSCs after treatment with the combination of TMZ and EMAP-II. BNIP3 overexpression strengthened the cytotoxic effects of EMAP-II and TMZ by inducing mitophagy. The combination of EMAP-II and TMZ decreased the expression of miR-24-3p, whose target gene was BNIP3. MiR-24-3p inhibited mitophagy and promoted proliferation, migration and invasion by down-regulating BNIP3 in GSCs. Furthermore, nude mice subjected to miR-24-3p silencing combined with EMAP-II and TMZ treatment displayed the smallest tumors and the longest survival rate. According to the above results, we concluded that EMAP-II enhanced the cytotoxic effects of TMZ on GSCs' proliferation, migration and invasion both *in vitro* and *in vivo*.

Keywords: GSCs, EMAP-II, TMZ, BNIP3, mitophagy

INTRODUCTION

Glioma is the most common primary invasive tumor of the central nervous system (Ostrom et al., 2015; Louis et al., 2016). The National Comprehensive Cancer Network (NCCN) Clinical Practice Guidelines state that the current standard of care with respect to glioma management includes surgical resection followed by radiotherapy with concomitant and adjuvant chemotherapy with

temozolomide (TMZ) (Stupp et al., 2005; Nabors, 2016). The anti-cancer effects of TMZ, an oral second-generation alkylating agent, are facilitated by its rapid hydrolysis into 5-(3-methyltriazen-1yl) imidazole-4-carboxamide (MITC) under physiological pH conditions (Pace et al., 2003). TMZ has been shown to confer more survival benefits than other chemotherapy drugs. However, the European Organization for Research and Treatment of Cancer/National Cancer Information Center (EORTC/NCIC) trial shows that the median survival time of patients treated with TMZ was 19 months, while the median survival time of patients treated without TMZ was 14.6 months (Rapp et al., 2015). Glioma stem cells (GSCs) are individual glioma founder cells with the capacity for infinite self-renewal and long-term proliferation, as well as the capacity for neurosphere formation and multipotential differentiation (Bao et al., 2006). It has been shown that GSCs is more resistant to conventional therapies than its differentiated counterpart. It has also proved that functional and some mechanistic evidence of the conversion of non-GSCs into GSCs both *in vitro* and *in vivo* after exposure to TMZ. Therefore One of the most significant impediments to the success of glioma chemotherapy is the presence of GSCs (Auffinger et al., 2014).

Endothelial-monocyte-activating polypeptide-II (EMAP-II) is a 22-kDa secretory polypeptide protein that was originally isolated from murine methylcholanthrene A-induced fibrosarcoma. It inhibits tumor angiogenesis and causes tumor cell apoptosis without effecting normal cells and thus has been applied in cancer therapy (Berger et al., 2000a,b). EMAP-II-induced autophagy has been shown to kill glioma cells and GSCs (Ma et al., 2015; Chen et al., 2016). Exogenous EMAP-II could enhance the synergic effects of bortezomib with gemcitabine by cleaving caspase-3 in pancreatic cancer cells (Awasthi et al., 2013). However, whether EMAP-II enhances the cytotoxic effects of TMZ on GSCs remains unknown.

The process of mitochondrial turnover predominantly comprises autophagic sequestration and the delivery of mitochondria to lysosomes for hydrolytic degradation, a phenomenon known as mitophagy (Tolkovsky et al., 2002; Devin and Rigoulet, 2007). Mitophagy is a process in which damaged mitochondria are degraded to maintain cell metabolic homeostasis. However, mitophagy may also entail the clearance of healthy mitochondria in response to hypoxia and starvation, causing cellular metabolic dysfunction and even cell death (Kanki and Klionsky, 2009; Kanki et al., 2009; Kurihara et al., 2012). Bcl-2/adenovirus E1B 19 kDa protein-interacting protein 3 (BNIP3) is a member of the Bcl-2 subfamily of death-inducing proteins and has been found to interact with adenoviruses E1B-19K (Bellot et al., 2009). BNIP3 affects mitophagy by interacting with mitochondria with BNIP3 transmembrane

domains (Zhang et al., 2008). It has been reported that TMZ can induce mitophagy in the U87 cell line (Lin et al., 2012), but the specific mechanism underlying this effect has not yet been elucidated. Whether TMZ exerts cytotoxic effect on GSCs though BNIP3-mediated mitophagy, as well as the mechanism though which TMZ exerts its effects, remain unclear.

MicroRNAs (miRNAs) are a family of endogenous, small (18–25 nucleotides) non-coding single-stranded RNA molecules found in all eukaryotic cells. Recent studies have shown that miRNAs can indirectly adjust autophagy, as well as mitophagy (Li et al., 2015). MiR-27a and miR-27b regulate autophagic clearance of damaged mitochondria by targeting PINK1 (Kim et al., 2016). MiR-24-3p has been found to be significantly overexpressed in oral squamous cell carcinoma (Lin et al., 2010) and promotes glioma cell proliferation (Xu et al., 2013). We found that EMAP-II induced upregulation of autophagy-related protein 5 (ATG5) and autophagy-related protein 7 (ATG7) to promote autophagy that killed glioma cells by down-regulating miR-20a(12). However, whether EMAP-II induces mitophagy in GSCs via miR-24-3p and enhances the cytotoxic effects of TMZ on GSCs has not been reported.

This study aims to verify whether low-dose EMAP-II enhances the cytotoxic effects of TMZ on GSCs and explores the mechanism by which EMAP-II induces BNIP3-dependent mitophagy via miR-24-3p down-regulation to enhance the inhibitory effects of TMZ on GSC malignant biological behavior.

MATERIALS AND METHODS

Cell Lines and Cell Culture

The human malignant glioma cell lines U-87 and U-251 and the human embryonic kidney cell line HEK293T were purchased from the Shanghai Institutes for Biological Sciences Cell Resource Center. All the cells were cultivated in DMEM supplemented with 10% fetal bovine serum (FBS, Life Technologies Corporation, Paisley, UK), and all the cells were incubated in a moist incubator at $37°C$ with 5% CO_2 and refreshed medium every 48 h.

De-Differentiation and Identification of GSCs

GSCs were isolated as described previously (Tu et al., 2013). U87 and U251cells were trypsinized using 0.05% trypsin/EDTA and supplemented with DMEM/F-12 (Life Technologies Corporation, Grand Island, NY, USA), basic fibroblast growth factor (bFGF, 10 ng/ml, Life Technologies Corporation, Carlsbad, CA, USA), epidermal growth factor (EGF, 10 ng/ml, Life Technologies Corporation, Gaithersburg, MD, USA) and 2% B27 (50×, Life Technologies Corporation, Grand Island, NY, USA). Fresh media was added every third day of culture and the cells were passaged when average neurosphere size reached ∼100–150 µm in diameter.

For differentiation experiments, spheres were dissociated by for a single cell suspension and seeded (2.5×10^4 cells/cm2) onto glass coverslips coated with poly-L-ornithine (BD Biosciences, Franklin Lakes, NJ, USA) in the medium without bFGF and EGF but containing 10 % FBS and were incubated for 7–11 days.

Abbreviations: EMAP-II, endothelial-monocyte-activating polypeptide-II; TMZ, temozolomide; GSCs, glioma stem cells; EORTC/NCIC, European Organization for Research and Treatment of Cancer/National Cancer Information Center; MITC, 5-(3-methyltriazen-1yl) imidazole-4-carboxamide; BNIP3, Bcl-2/adenovirus E1B 19 kDa protein-interacting protein 3; ATG5, autophagy-related protein 5; ATG7, autophagy-related protein 7; EGF, epidermal growth factor; bFGF, basic fibroblast growth factor; FBS, fetal bovine serum; IDVs, integrated density values; NCCN, National Comprehensive Cancer Network.

For immunofluorescence staining of undifferentiated spheres, cells were incubated with antibodies against Nestin and CD133 (1:100, Santa Cruz Biotechnology, Santa Cruz, CA, USA). For immunostaining of differentiated spheres, cells were stained with antibodies against GFAP (1:100, Abcam, Cambridge, MA, USA) and beta-tubulin III (1:100, Santa Cruz Biotechnology). The primary antibody complexes were visualized with anti-rabbit Alexa Fluor 488 and anti-mouse Alexa Fluor 555 secondary antibodies (Beyotime Institute of Biotechnology, Jiangsu, China). Nuclei were counterstained with $4'$, 6-diamidino-2-phenylindole (DAPI).

Experimental Groups

1. To investigate the effects of EMAP-II and TMZ on U87-GSCs and U251-GSCs, we divided the cells into the following four groups ($n = 3$): (1) Control group, whose cells were treated with 0.9% sodium chloride (NS); (2) EMAP-II group, whose cells were treated with 0.05 nM EMAP-II for 0.5 h; (3) TMZ group, whose cells were treated with $400\,\mu M$ TMZ for 48 h; and (4) EMAP-II+TMZ group, whose cells were treated with $400\,\mu M$ TMZ for 48 h after pretreatment with 0.05 nM EMAP-II for 0.5 h.

2. To investigate whether BNIP3-mediated mitophagy was involved in regulating GSCs, we divided the cells into the following five groups ($n = 3$): (1) Control group; (2) BNIP3(+)NC group, whose cells were transfected with a negative-control (NC) BNIP3-overexpressing plasmid; (3) BNIP3(+) group, whose cells were transfected with a BNIP3 overexpressing plasmid; (4) BNIP3(−)NC group, whose cells were transfected with an NC BNIP3-silencing plasmid; and (5) BNIP3(−) group, whose cells were transfected with a BNIP3-silencing plasmid.

3. To investigate whether BNIP3 participated in the effects exerted by the combination of EMAP-II and TMZ on GSCs, we divided the cells into the following four groups ($n = 3$): (1) Control group; (2) EMAP-II+TMZ group, whose cells were treated with $400\,\mu M$ TMZ for 48 h after pretreatment with 0.05 nM EMAP-II for 0.5 h; (3) BNIP3(+)+EMAP-II+TMZ group, whose BNIP3-overexpressing cells were treated with $400\,\mu M$ TMZ for 48 h after pretreatment with 0.05 nM EMAP-II for 0.5 h; and (4) BNIP3(−)+EMAP-II+TMZ group, whose BNIP3-silenced cells were treated with $400\,\mu M$ TMZ for 48 h after pretreatment with 0.05 nM EMAP-II for 0.5 h.

4. To study the effects of miR-24-3p on mitophagy in GSCs, we divided the cells into the following five groups ($n = 3$): (1) Control group; (2) Agomir-24-3p-NC group, whose cells were transfected with an NC miR-24-3p agomir; (3) Agomir-24-3p group, whose cells were transfected with a miR-24-3p agomir; (4) Antagomir-24-3p-NC group, whose cells were transfected with an NC miR-24-3p antagomir; and (5) Antagomir-24-3p group, whose cells were transfected with a miR-24-3p antagomir.

5. To investigate whether whether miR-24-3p could play a role in regulating BNIP3 in the combination of EMAP-II and TMZ, we divided the cells into the following four groups ($n = 3$):(1) Control group; (2) EMAP-II+TMZ group, whose cells were treated with $400\,\mu M$ TMZ for 48 h after pretreatment with 0.05 nM EMAP-II for 0.5 h; (3) agomir-24-3p+EMAP-II+TMZ group, whose agomir-24-3p cells were treated with $400\,\mu M$ TMZ for 48 h after pretreatment with 0.05 nM EMAP-II for 0.5 h; and (4) antagomir-24-3p+EMAP-II+TMZ group, whose antagomir-24-3p cells were treated with $400\,\mu M$ TMZ for 48 h after pretreatment with 0.05 nM EMAP-II for 0.5 h.

6. To study the effects of miR-24-3p and BNIP3 on mitophagy, we divided the cells into the following nine groups ($n = 3$): (1) Control group; (2) Agomir-24-3p-NC+BNIP3(+) NC group, whose cells were transfected with an NC miR-24-3p agomir and a BNIP3-overexpressing plasmid; (3) Agomir-24-3p+BNIP3(+) group, whose cells were transfected with a miR-24-3p agomir and BNIP3 overexpressing plasmid; (4) Agomir-24-3p-NC+BNIP3(-) NC group, whose cells transfected with an NC miR-24-3p agomir and a BNIP3-silencing plasmid; (5) Agomir-24-3p+BNIP3(−) group, whose cells were transfected with a miR-24-3p agomir and BNIP3 silencing plasmid; (6) Antagomir−24-3p-NC+BNIP3(+)-NC group, whose cells were transfected with an NC miR-24-3p antagomir and a BNIP3 overexpressing plasmid; (7) Antagomir-24-3p+BNIP3(+) group, whose cells were transfected with a miR-24-3p antagomir and BNIP3 overexpressing plasmid; (8) Antagomir−24-3p-NC+BNIP3(–) group, whose cells were transfected with an NC miR-24-3p antagomir and a BNIP3-silencing plasmid; and (9) Antagomir-24-3p+BNIP3(–) group, whose cells were transfected with a miR-24-3p antagomir and BNIP3-silencing plasmid.

Cell Viability Assay

Cell Counting Kit-8 (CCK8, Dojindo, Tokyo, Japan) was used for cell cytotoxicity and proliferation assay. Cells were seeded in 96-well plates at a density of 5,000 cells per well, and 10 µl of CCK8 was added into each well at 24, 48, 72 h after DMSO or TMZ treatment (0, 100, 200, 400, 600, 800, 1000, 1200 µM). As the cells incubated at 37°C for 4 h, the absorbance was measured at a wave length of 450 nm every 30 min.

Cell Migration and Invasion Assay

Cell migration and invasion was measured using a transwell permeable chamber (6.5 mm in diameter, 8 µm pore size, Corning Incorporate, Corning, NY, USA). Cells were suspended in 100 µl of serum-free medium and then added to the upper chamber (without Matrigel for cell migration assay) or seeded in a Matrigel-pre-coated upper chamber (for cell invasion assay), while 500 µl of medium with 10% FBS was added to the lower chamber. Then, the medium in the lower chamber was replaced with 500 µl of 10% FBS medium. After incubation for 24 h, the cells that had migrated to or invaded the bottom of the membrane were fixed with methanol/glacial acetic acid mixture for 30 min and then stained with 10% Giemsa. Then the pictures of stained cells were taken with an inverted microscope. And the cell number in three randomly fields were counted. Data were collected from repeated three independent experiments.

Cell Transfection

The human BNIP3 gene was ligated into a pGCMV/MCS/IRES/EGFP/Neo vector (GenePharma, Shanghai, China) to construct a BNIP3(+) plasmid, and the shRNA sequence against BNIP3 was ligated into a pGPU6/GFP/Neo vector. The U87 and U251 cell lines were transfected with BNIP3(+)-encoding plasmids or BNIP3 shRNA and designated BNIP3(+) cells or BNIP3(−) cells, respectively. Empty vectors were used for the negative controls (NCs). Opti-MEM and Lipofectamine 3000 reagent (Life Technologies Corporation, Carlsbad, CA, USA) were used according to the manufacturer's instructions. Transfection was performed at about 80% confluency of cells in 24-well plates with Opti-MEM® I and Lipofectamine 3,000 reagent. Stable cell lines were obtained through selection using 0.4 mg/ml geneticin (G418; Sigma-Aldrich, St Louis, MO, USA). Geneticin-resistant cells were obtained after 4 or 5 weeks. Geneticin-resistant GSCs were subsequently isolated from these cells.

The cells were transfected with a miR-24-3p agomir, miR-24-3p antagomir, or the appropriate NC (GenePharma, Shanghai, China) using Lipofectamine 3,000 reagent (Life Technologies Corporation), according to the manufacturer's instructions. After 6 h of transfection, the medium was removed and replaced with fresh medium. The cells were harvested after 48 h of transfection.

Immunofluorescence Staining

Cells were stained with LysoTracker Red or MitoTracker Red at a final concentration of 50 nM. Then, the cells were fixed in 4% paraformaldehyde for 30 min, blocked with 5% BSA for 2 h, and incubated with the primary antibody for microtubule-associated protein one light chain 3 (LC3, 1:150, Abcam, Cambridge, MA, USA, ab51520) at 4°C overnight. Then, the cells were washed and incubated with the appropriate secondary antibody before being counterstained with DAPI (Beyotime Institute of Biotechnology, Jiangsu, China) for 10 min and visualized with a confocal microscope.

Luciferase Reporter Assays

For the luciferase reporter assays, HEK-293T cells were seeded into 96-well plates. These cells were co-transfected with a wild-type (Wt) or mutant (Mut) pmirGLO-BNIP3 reporter plasmid and an agomir-24-3p or agomir-24-3p-NC. After 48 h, luciferase activity was measured using Dual-luciferase Reporter Assay System (Promega, Madison, WI, USA). Relative firefly luciferase activity levels were calculated and normalized to that of renilla luciferase.

RNA Extraction and Quantitative RT-PCR (qRT-PCR)

Total RNA was separated from U87-GSCs and U251-GSCs using Trizol reagent (Life Technologies Corporation). A Taq-Man MicroRNA Reverse Transcription Kit was used for miRNA reverse transcription (Applied Biosystems, Foster City, CA, USA). QRT-PCR was performed using TaqMan Universal Master Mix II with Taq-Man microRNA assays for miR-24-3p and U6 expression. For quantification of BNIP3 mRNA, we performed reverse transcription and RT-PCR amplification using an RT-PCR kit and SYBR Premix Dimer Eraser (TaKaRa, Dalian, China) and the assays for BNIP3 and GAPDH gene expression (Applied Biosystems). Fold changes were calculated using the relative quantification $(2^{-\Delta\Delta Ct})$ method.

Western Blot Analysis

U87-GSCs and U251-GSCs were lysed using ice-cold RIPA buffer and centrifuged at $17,000 \times$ g at 4°C for 40 min. Protein concentrations were determined by a BCA Protein Assay Kit (Beyotime Institute of Biotechnology, Jiangsu, China). The proteins (30–60 μg) were separated by 10–15% SDS-PAGE and transferred onto PVDF membranes, which were blocked with 5% non-fat milk for 2 h and then incubated overnight with primary antibodies against LC3 (1:1000, Abcam, Cambridge, MA, USA, ab51520), P62/SQSTM1 (1:1000, Proteintech, Chicago, IL, USA, ab56416), GAPDH(1:10,000, Proteintech, Chicago, IL, USA, 6000-4-Ig), BNIP3 (1:1000, Abclonal, Cambridge, MA, USA, A5683), TOMM20 (1:1000, Proteintech, Chicago, IL, USA, 11802-1-AP), and CYPD (1:1000, Proteintech, Chicago, IL, USA, 12716-1-AP). After being washed with TBST, the membranes were incubated with the appropriate secondary antibodies. The protein bands were visualized with an enhanced chemiluminescence (ECL) kit (Santa Cruz Biotechnology) and scanned with ChemImager 5500 V2.03 Software. The relative integrated density values (IDVs) were calculated using FluorChem 2.0 software and normalized to those of GAPDH.

Subcutaneous and Orthotopic Xenografts in Nude Mice

Stably transfected U87-GSCs and U251-GSCs cells were used in the *in vivo* study. A lentivirus encoding a miR-24-3p silencer was generated using a pLenti6.3/V5eDEST Gateway Vector Kit (Life Technologies Corporation, Carlsbad, CA, USA). The miR-24-3p silencer was ligated into the pLenti6.3/V5eDEST vector (GenePharma, Shanghai, China), and then a pLenti6.3/V5eDEST-miR-24-3p-silencing vector was generated. The lentivirus was generated in 293FT cells using ViraPower Packaging Mix. After infection, the cells that stably expressed the miR-24-3p-silencer [miR-24-3p(−)] were selected.

Athymic nude mice (BALB/C-nu/nu, 4 weeks old, male) were purchased from the Cancer Institute of the Chinese Academy of Medical Science. The ethics committee of Shengjing Hospital has approved this study. The animals were raised in accordance with the guidelines of the Laboratory Animal Centre. The cells were subcutaneously implanted into the right flanks of the mice at a density of 5×10^5 cells/mouse ($n = 10$ each group). Tumor volumes were measured every 5 days until 50 days post-inoculation and were calculated using the following formula: volume (mm^3) = length × width^2/2.

For intracranial orthotopic inoculation, 3×10^5 cells were stereotactically implanted in the right striatum of the mice ($n = 10$ each group). Mice died within 7 days post-operation were considered to have unrelated to tumors and eliminated from the study. New mice were then treated and added to the

groups. The numbers of surviving mice were recorded daily until 50 days post-operation. Survival analysis was performed using Kaplan-Meier survival curves. Tumor-bearing mice were divided into the following four groups: (1) Control group, whose mice treated with 0.9% sodium chloride; (2) EMAP-II+TMZ group, whose mice were treated with 400 μM TMZ after pretreatment with 0.05 nM EMAP-II for 0.5 h; (3) miR-24-3p(−) group, whose mice were treated with cells stably expressing miR-24-3p(−); (4) EMAP-II+TMZ+miR-24-3p(−) group, whose mice were treated with cells stably expressing miR-24-3p(−) and 400 μM TMZ after pretreatment with 0.05 nM EMAP-II for 0.5 h.

Transmission Electron Microscopy (TEM)

The cells were fixed in 2.5% glutaraldehyde (electron microscopy grade) in phosphate-buffered saline (PBS) at 4°C for 2 h, dehydrated in an ethanol series and embedded in Epon resin. Ultrathin sections were then subjected to TEM analysis. Representative areas were chosen for ultrathin sectioning and viewed with a Philips EM 400 transmission electron microscope at an accelerating voltage of 80 kV, and digital images were obtained by an AMT imaging system (Advanced Microscopy Techniques Cor, Danvers, MA, USA).

Statistical Analysis

Data are presented as the mean ± standard deviation (SD) and were analyzed using SPSS19.0 (SPSS, IL, USA). Statistical analysis was performed using Student's t-test and one-way ANOVA. $P < 0.05$ was considered statistically significant. IC50 was measured by GraphPad Prism software (raw data in Data Sheet 1).

RESULTS

De-Differentiation and Identification of GSCs

The result we already published showed that the isolated GSCs using sphere culture by flow cytometry analysis contained 98.2 and 98.6% CD133+ cells in GSCs-U251 and GSCs-U87, respectively (Zhang et al., 2013). To identify GSCs, we use immunofluorescence staining. The positive staining of Nestin and CD133 confirmed that most cells within the spheres expressed these neural stem cell lineage markers on their membranes (**Supplementary Figure 1A**). Besides, the cell spheres are differentiated into a non-GSC line in DMEM supplemented with 10% FBS, without EGF or FGF. These cells showed typical morphological differentiation toward neuronal and astrocytic lineages, identified as beta-tubulin-III positive neurons and GFAP-positive astrocytes (**Supplementary Figure 1B**).

EMAP-II Intensified the Suppressive Effects of TMZ on U87-GSCs and U251-GSCs Viability, Migration, and Invasion

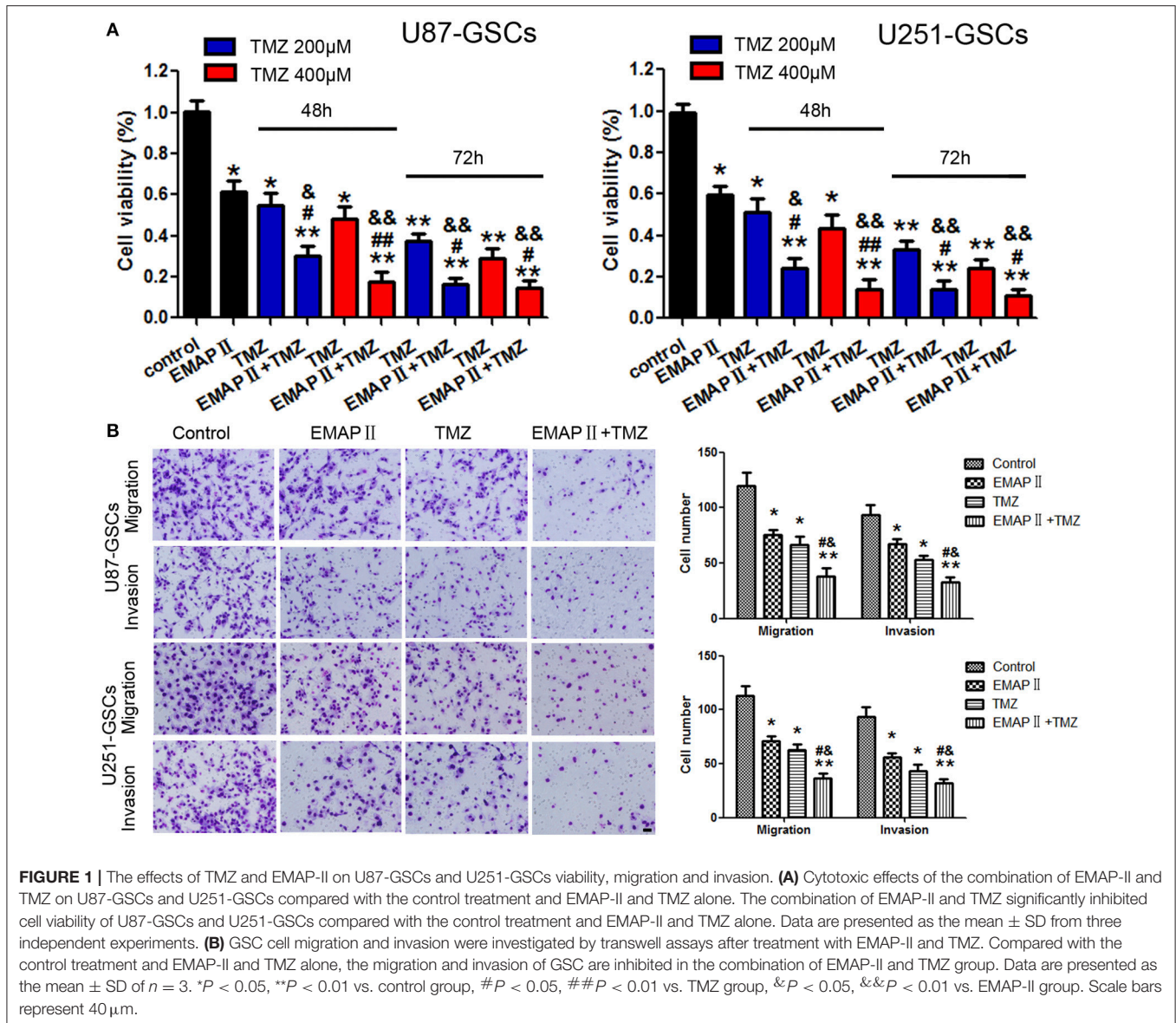The cytotoxicity of TMZ and EMAP-II was measured by Cell Counting Kit-8 (CCK-8).Based on the IC50 values of TMZ

against U87-GSCs and U251-GSCs (Zhou et al., 2017), we selected the concentrations of 200 and 400 μM and the time periods of 48 or 72 h for subsequent experiments. According to the results of our preliminary study (Chen et al., 2016), 0.05 nM EMAP-II and 0.5 h were selected as the optimum pretreatment concentration and time point, respectively. Viability was apparently inhibited in the EMAP-II and TMZ groups and the EMAP-II and TMZ combination group after 48 and 72 h of treatment ($P < 0.05$, $P < 0.05$, $P < 0.01$). Compared with the EMAP-II and TMZ groups, the EMAP-II and 200 and 400 μM TMZ combination groups displayed significantly reduced cell viability after 48 h of treatment ($P < 0.05$, $P < 0.01$). The EMAP-II and 200 or 400 μM TMZ combination groups also displayed significantly lower cell viability than the EMAP-II group after 72 h of treatment ($P < 0.05$; **Figure 1A**). Thus, 0.05 nM EMAP-II for 0.5 h and 400 μM TMZ for 48 h were the pretreatment and treatment concentrations and times, respectively, used in subsequent experiments.

Next we explore the combination of EMAP-II and TMZ on migration and invasion of GSCs.U87-GSC and U251-GSC migration and invasion were significantly inhibited in the EMAP-II and TMZ groups and the EMAP-II and TMZ combination group ($P < 0.05$). Compared with the EMAP-II and TMZ groups, the EMAP-II and TMZ combination group displayed significantly decreased migration and invasion ($P < 0.05$; **Figure 1B**).

Combination Treatment With EMAP-II and TMZ Induced Mitophagy in GSCs

TEM and Immunofluorescence assay was used to monitor mitophagy. Autophagysome activity levels were increased in the EMAP-II and TMZ groups and the EMAP-II and TMZ combination group. The EMAP-II and TMZ combination group displayed more autophagysomes than the EMAP-II and TMZ groups (**Figure 2A**). U87-GSC and U251-GSC were stained for LC3 (green) and Mito-Tracker or Lyso-Tracker (red). The punctate density and distribution indicates LC3 expression. LC3 punctuate staining was increased in the EMAP-II and TMZ groups and the EMAP-II and TMZ combination group. LC3 punctuate staining was dramatically increased in the EMAP-II and TMZ combination group compared with the EMAP-II and TMZ groups. Additionally, we noted an overlap between LC3 and Mito-Tracker or Lyso-Tracker. The latter two agents exhibited a staining trend similar to that of LC3, and their dots colocalized with the LC3 dots (**Figures 2B,C**).

Western blot was used to detect the protein expression of LC3 II/I, P62, mitochondrial matrix protein CYPD and mitochondrial membrane protein TOMM20 in U87-GSCs and U251-GSCs. The LC3-II/I ratio gradually increased in the EMAP-II and TMZ groups and the EMAP-II and TMZ combination group ($P < 0.01$), but P62, TOMM20 and CYPD expression levels displayed gradual decreases in the EMAP-II and TMZ groups and the EMAP-II and TMZ combination group ($P < 0.05$). The LC3-II/I ratio increased ($P < 0.05$), but P62, TOMM20 and CYPD expression levels decreased in the EMAP-II and

FIGURE 1 | The effects of TMZ and EMAP-II on U87-GSCs and U251-GSCs viability, migration and invasion. **(A)** Cytotoxic effects of the combination of EMAP-II and TMZ on U87-GSCs and U251-GSCs compared with the control treatment and EMAP-II and TMZ alone. The combination of EMAP-II and TMZ significantly inhibited cell viability of U87-GSCs and U251-GSCs compared with the control treatment and EMAP-II and TMZ alone. Data are presented as the mean ± SD from three independent experiments. **(B)** GSC cell migration and invasion were investigated by transwell assays after treatment with EMAP-II and TMZ. Compared with the control treatment and EMAP-II and TMZ alone, the migration and invasion of GSC are inhibited in the combination of EMAP-II and TMZ group. Data are presented as the mean ± SD of $n = 3$. *$P < 0.05$, **$P < 0.01$ vs. control group, #$P < 0.05$, ##$P < 0.01$ vs. TMZ group, &$P < 0.05$, &&$P < 0.01$ vs. EMAP-II group. Scale bars represent 40 μm.

TMZ combination group compared with the EMAP-II and TMZ groups ($P < 0.05$; **Figure 2D**).

Combination Treatment With EMAP-II and TMZ Inhibited GSCs Malignant Behavior by Upregulating BNIP3

EMAP-II and TMZ influenced the expression of BNIP3 in GSCs. BNIP3 protein expression increased significantly in the EMAP-II and TMZ groups and the EMAP-II and TMZ combination group ($P < 0.05$). BNIP3 protein expression increased in the EMAP-II and TMZ combination group compared with EMAP-II and TMZ groups ($P < 0.05$) (**Figure 3A**). Proliferation, migration, and invasion of GSCs were influenced by BNIP3 overexpression and knockdown. GSCs proliferation, migration, and invasion were inhibited in the BNIP3(+) group ($P < 0.05$) and were enhanced in the BNIP3(-) group ($P<0.05$) (**Figures 3B,C**).

Combination Treatment of EMAP-II and TMZ Induced Mitophagy by Up-Regulating BNIP3

We furtherly analyzed the effect of BNIP3 on mitophagy in GSCs. The LC3-II/I ratio and BNIP3 expression increased ($P < 0.01$, $P < 0.05$), but the expression levels of P62, TOMM20 and CYPD decreased in the BNIP3(+) group ($P < 0.01$, $P < 0.05$). Consistent with these findings, the LC3-II/I ratio and BNIP3 expression decreased ($P < 0.01$), and P62, TOMM20 and CYPD expression levels increased in the BNIP3(-) group ($P < 0.01$) ($P < 0.05$) (**Figure 4A**).

To explore whether BNIP3 displayed an important role in the combination of EMAP-II and TMZ, GSCs were treated with EMAP-II and TMZ based on whether BNIP3 was overexpressed or knocked down. The LC3II/I ratio and BNIP3 expression was increased ($P < 0.05$), but P62,
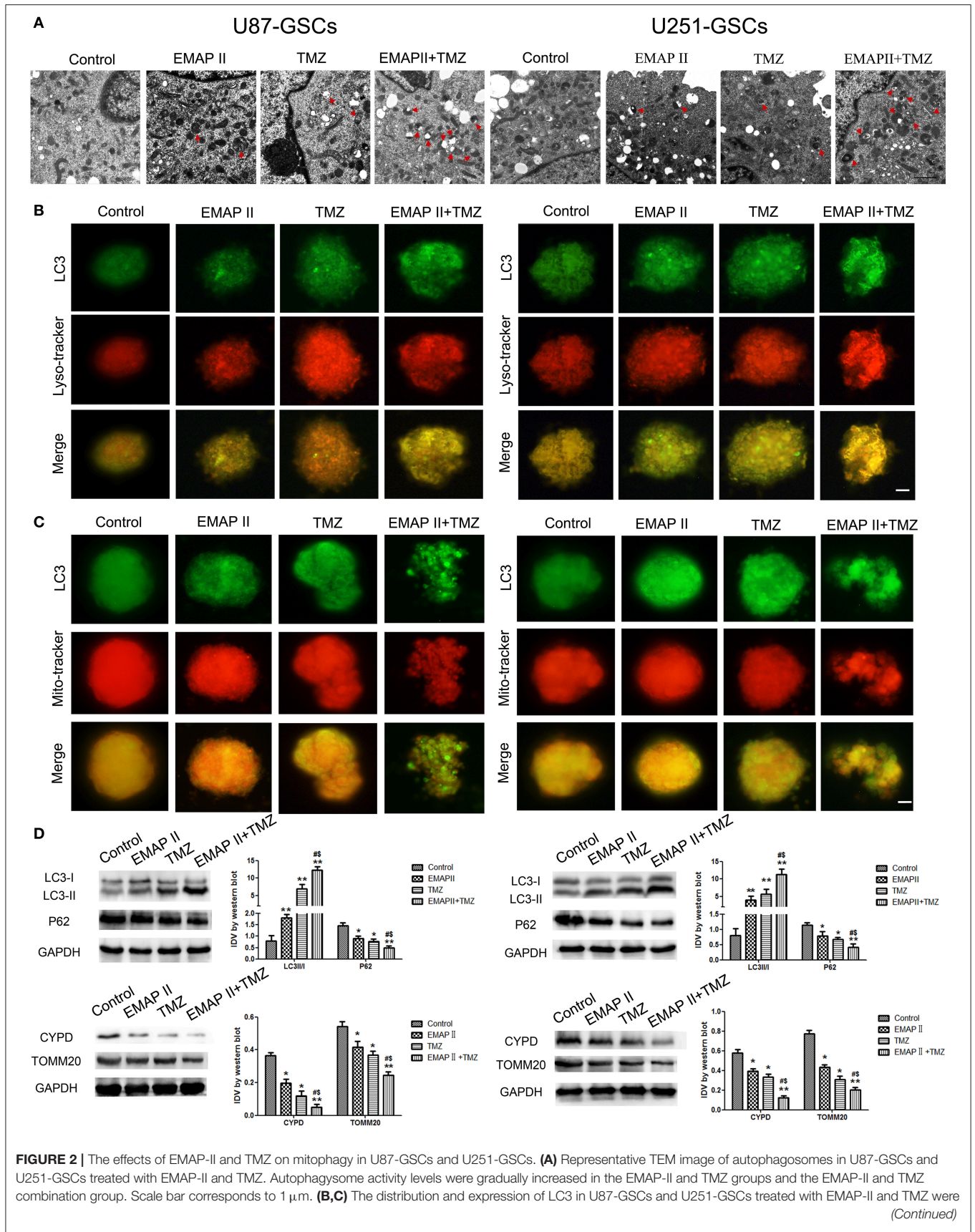
FIGURE 2 | The effects of EMAP-II and TMZ on mitophagy in U87-GSCs and U251-GSCs. **(A)** Representative TEM image of autophagosomes in U87-GSCs and U251-GSCs treated with EMAP-II and TMZ. Autophagysome activity levels were gradually increased in the EMAP-II and TMZ groups and the EMAP-II and TMZ combination group. Scale bar corresponds to 1 μm. **(B,C)** The distribution and expression of LC3 in U87-GSCs and U251-GSCs treated with EMAP-II and TMZ were

(Continued)

FIGURE 2 | analyzed by immunofluorescence assay with Lyso-Tracker and Mito-Tracker. The expression of LC3 indicates the occurrence of autophagy. The distribution of LC3 that overlap with lysosome or mitochondria indicates autophagy or mitophagy. Scale bars represent 20 μm. **(D)** Western blot analysis of the LC3-II/I ratio and P62, TOMM 20, and CYPD expression levels in U87-GSCs and U251-GSCs treated with EMAP-II and TMZ. The LC3-II/I ratio increased, but P62, TOMM 20, and CYPD expression decreased in GSCs treated with EMAP-II and TMZ. Data are presented as the mean ± SD of $n = 3$. $*P < 0.05$, $**P < 0.01$ vs. control group, $^\#P < 0.05$ vs. TMZ group, $^\&P < 0.05$ vs. EMAP-II group.
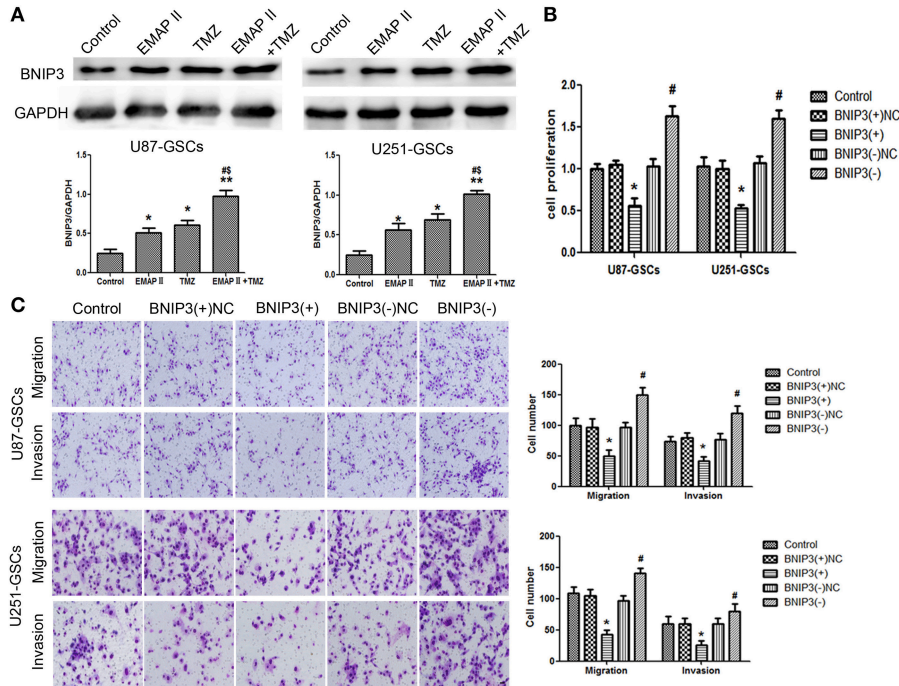
FIGURE 3 | The effects of BNIP3 on GSC malignant behavior in U87-GSCs and U251-GSCs treated with EMAP-II and TMZ. **(A)** Effects of EMAP-II and TMZ on BNIP3 expression in U87-GSCs and U251-GSCs, as demonstrated by western blotting. The combination of EMAP-II and TMZ significantly increased the level of BNIP3 expression. Data are presented as the mean ± SD of $n = 3$. $*P < 0.05$, $**P < 0.01$ vs. control group, $^\#P < 0.05$ vs. TMZ group, $^\&P < 0.05$ vs. EMAP-II group. **(B)** The effects of BNIP3 on U87-GSC and U251-GSC proliferation were assessed by CCK-8. BNIP3 overexpression inhibited GSC proliferation. Data are presented as the mean ± SD of $n = 3$. $*P < 0.05$ vs. BNIP3(+)-NC group, $^\#P < 0.05$ vs. BNIP3(−)-NC group. **(C)** The effects of BNIP3 on U87-GSC and U251-GSC migration and invasion were assessed by transwell assays. BNIP3 overexpression inhibited GSC migration and invasion. Data are presented as the mean ± SD of $n = 3$. $*P < 0.05$, vs. BNIP3(+)-NC group, $^\#P < 0.05$ vs. BNIP3(−)-NC group.

TOMM20, and CYPD expression levels were decreased in the BNIP3(+)+EMAP-II+TMZ group compared with the EMAP-II and TMZ combination group ($P < 0.05$). The opposite result was observed in the BNIP3(−)+EMAP-II+TMZ group compared with the EMAP-II and TMZ combination group (**Figure 4B**). GSCs proliferation, migration and invasion were increased in the BNIP3(−)+EMAP-II+TMZ group compared with EMAP-II and TMZ combination group ($P < 0.05$) and were inhibited in the BNIP3(+)+EMAP-II+TMZ group compared with EMAP-II and TMZ combination group ($P < 0.05$; **Figures 4C,D**).

Combination Treatment With EMAP-II and TMZ Induced Mitophagy and Inhibited GSC Malignant Behavior by Down-Regulating miR-24-3p

The expression level of miR-24-3p in GSCs was detected by real-time PCR. MiR-24-3p expression levels were decreased in

the EMAP-II and TMZ groups and the EMAP-II and TMZ combination group ($P < 0.05$). MiR-24-3p expression levels were decreased in the EMAP-II and TMZ combination group compared with the EMAP-II and TMZ groups ($P < 0.05$; **Figure 5A**).

Mitophagy-related proteins were affected by miR-24-3p. The LC3-II/I ratio and BNIP3 protein expression were decreased ($P < 0.05$), but P62, TOMM20, and CYPD expression levels were increased in the Agomir-24-3p group compared with the corresponding Control group ($P < 0.05$). Conversion of LC3-I to LC3-II and BNIP3 protein expression were increased ($P < 0.05$), but P62, TOMM20, and CYPD expression levels were decreased in the Antagomir-24-3p group compared with the corresponding Control group ($P < 0.05$) (**Figures 5B,C**). GSC proliferation, migration and invasion were inhibited in the Antagomir-24-3p group compared with the corresponding Control group ($P < 0.05$) and were enhanced in the Agomir-24-3p group compared with the corresponding Control group ($P < 0.05$; **Figures 5D,E**).
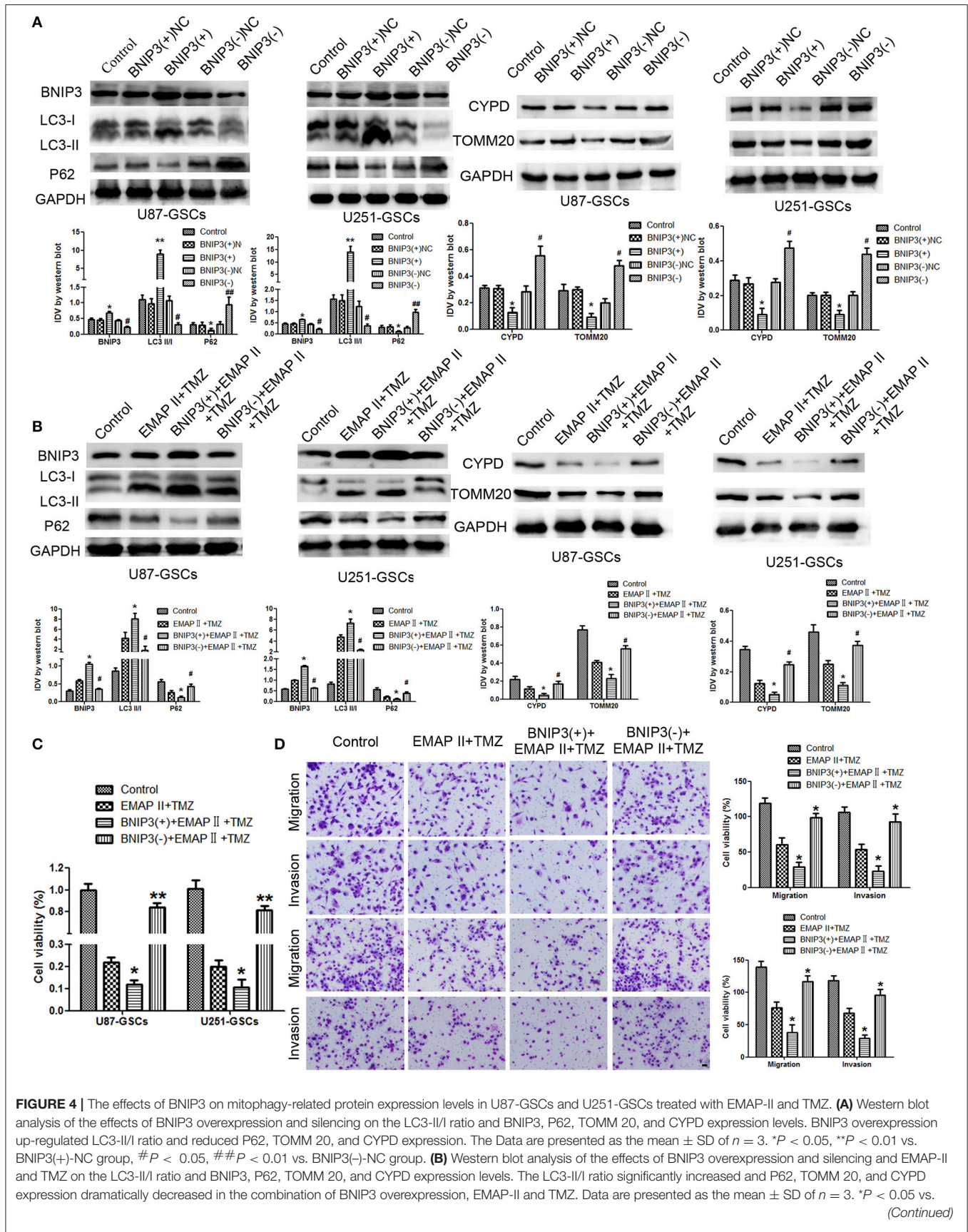
FIGURE 4 | The effects of BNIP3 on mitophagy-related protein expression levels in U87-GSCs and U251-GSCs treated with EMAP-II and TMZ. **(A)** Western blot analysis of the effects of BNIP3 overexpression and silencing on the LC3-II/I ratio and BNIP3, P62, TOMM 20, and CYPD expression levels. BNIP3 overexpression up-regulated LC3-II/I ratio and reduced P62, TOMM 20, and CYPD expression. The Data are presented as the mean ± SD of $n = 3$. *$P < 0.05$, **$P < 0.01$ vs. BNIP3(+)-NC group, #$P < 0.05$, ##$P < 0.01$ vs. BNIP3(–)-NC group. **(B)** Western blot analysis of the effects of BNIP3 overexpression and silencing and EMAP-II and TMZ on the LC3-II/I ratio and BNIP3, P62, TOMM 20, and CYPD expression levels. The LC3-II/I ratio significantly increased and P62, TOMM 20, and CYPD expression dramatically decreased in the combination of BNIP3 overexpression, EMAP-II and TMZ. Data are presented as the mean ± SD of $n = 3$. *$P < 0.05$ vs.

(Continued)

FIGURE 4 | EMAP-II+TMZ group, $^{\#}P < 0.05$ vs. EMAP-II+TMZ group.(C,D) CCK8 and transwell assays of the effects of BNIP3 overexpression or silencing and the combination of EMAP-II and TMZ on the proliferation, migration, and invasion of U87-GSCs and U251-GSCs. The combination of BNIP3 overexpression, EMAP-II and TMZ inhibited GSCs proliferation, migration, and invasion. Data are presented as the mean ± SD of $n = 3$. *$P < 0.05$ vs. EMAP-II+TMZ group, $^{\#}P < 0.05$, **$P < 0.01$ vs. EMAP-II+TMZ group. Scale bars represent 40 μm.

BNIP3 Was the Target Gene of miR-24-3p

By using TargetScan Human Release 6.2 Software, there was a potential binding site between miR-24-3p and 3'-UTR of BNIP3. Dual-luciferase gene reporter assay proved luciferase activity was significantly decreased in the Wt BNIP3 3' untranslated region (3'UTR)+agomir-24-3p group ($P < 0.05$). There was no significant difference in luciferase activity between the Mut BNIP3 3'UTR+agomir-24-3p-NC group and Mut BNIP3 3'UTR+agomir-24-3p group ($P > 0.05$; **Figure 6A**).

BNIP3 mRNA expression levels were not significantly different between the treated groups and their respective control groups ($P > 0.05$) (**Figure 6B**).

To furtherly explore whether miR-24-3p could affect BNIP3 in the combination of EMAP-II and TMZ, GSCs were treated with EMAP-II and TMZ on the basis of over-express or down-regulate miR-24-3p. Compared with EMAP-II+TMZ group, the expression of BNIP3 was reduced in agomir-24-3p+ EMAP-II+TMZ group; the expression of BNIP3 was increased in antagomir-24-3p+EMAP-II+TMZ group (**Figure 6C**).

BNIP3-Mediated Mitophagy Influenced GSC Malignant Behavior by Down-Regulating miR-24-3p

The expression of mitophagy-related proteins was affected by cotransfection of BNIP3 and miR-24-3p. No significant differences in LC3II/I, P62, TOMM20, and CYPD expression levels were detected in the Agomir-24-3p+BNIP3(+) and Antagomir-24-3p+BNIP3(−) groups compared with the corresponding Control groups ($P > 0.05$). The LC3-II/I ratio was decreased ($P < 0.05$), but P62, TOMM20 and CYPD expression levels were increased in the Agomir-24-3p+BNIP3(−) group ($P < 0.05$, $P < 0.01$, $P < 0.01$). Conversion of LC3-I to LC3-II was increased ($P < 0.01$), but P62, TOMM20, and CYPD expression levels were decreased in the Antagomir-24-3p+BNIP3(+) group ($P < 0.01$) (**Figures 7A,B**).

GSC proliferation, migration and invasion were enhanced in the Agomir-24-3p+BNIP3(−) group ($P < 0.05$). The opposite results were noted in the Antagomir-24-3p+BNIP3(+) group ($P < 0.05$) (**Figures 7C,D**).

The Combination of miR-24-3p, EMAP-II and TMZ Inhibited Tumor Growth in Vivo by Inducing BNIP3-Mediated Mitophagy

To prove the above findings, the growth-inhibitory effect of EMAP-II, TMZ and miR-24-3p inhibitor on U87-GSCs and U251-GSCs was tested in xenografted mice. The tumor volumes of the xenografts were significantly smaller in the EMAP-II+TMZ, miR-24-3p(−) and miR-24-3p(−)+EMAP-II+TMZ

groups than in the Control group. The tumor volume of EMAP-II+TMZ group is smaller than that of the EMAP-II and the TMZ group. The minimum volume was noted in the miR-24-3p(−)+EMAP-II+TMZ group (**Figures 8A–C**). Mouse survival time were much longer in the EMAP-II+TMZ, miR-24-3p(−) and miR-24-3p(−)+EMAP-II+TMZ groups than in the Control group. Mouse survival time was significantly longer in the miR-24-3p(−)+EMAP-II+TMZ group than in the other groups (**Figure 8D**).

In addition, we explore the molecular changes in tumor tissues. Compared with control group, The LC3-II/I ratio and BNIP3 expression was increased ($P < 0.05$, $P < 0.05$), but P62, TOMM20 and CYPD expression levels were decreased in the EMAP-II+TMZ, miR-24-3p(−) and miR-24-3p(−)+EMAP-II+TMZ groups [$P < 0.05$, $P < 0.05$, $P < 0.05$).Compared with the EMAP-II+TMZ, miR-24-3p(−) group, The LC3-II/I ratio and BNIP3 expression was increased ($P < 0.05$, $P < 0.05$)], but P62, TOMM20 and CYPD expression levels were decreased in miR-24-3p(−)+EMAP-II+TMZ group($P < 0.05$, $P < 0.05$, $P < 0.05$). All the results show that miR-24-3p-BNIP3- mitophagy is related with xenografted tumor growth. (**Supplementary Figure 2**).

DISCUSSION

We found that EMAP-II enhanced the cytotoxic effects of TMZ on GSC viability, migration and invasion. The combination of TMZ and EMAP-II induced GSC mitophagy, which was shown to inhibit GSC malignant behavior by upregulating BNIP3-mediated mitophagy. We also found that the combinaltion of TMZ and EMAP-II decreased miR-24-3p expression and that BNIP3 was the target gene of miR-24-3p. The combination of TMZ and EMAP-II induced mitophagy to inhibit malignant GSC behavior by down-regulating miR-24-3p. The results of our experiments with the xenografted mice showed that the EMAP-II+TMZ, miR-24-3p(−) and miR-24-3p(−)+EMAP-II+TMZ groups had smaller tumors and longer survival times than the other groups. In particular, the miR-24-3p(−)+EMAP-II+TMZ group had the smallest tumors and the longest survival time.

TMZ resistance is one of the major problems in chemotherapy. Some potential mechanisms underlying this resistance have been reported, including O6-methylguanine-DNA-methyltransferase (*MGMT*) expression, GSC microenvironment-induced resistance and autophagy-induced resistance (Kanzawa et al., 2004; Singh et al., 2004; Ohka et al., 2012). GSCs are less sensitive to chemotherapy than glioma cells, which is one of the reasons why the above chemotherapy has only limited effectiveness in those cells (Yu et al., 2015). In our previous study which has different mechanism with our recent study (Zhou et al., 2017), we found that GSC viability
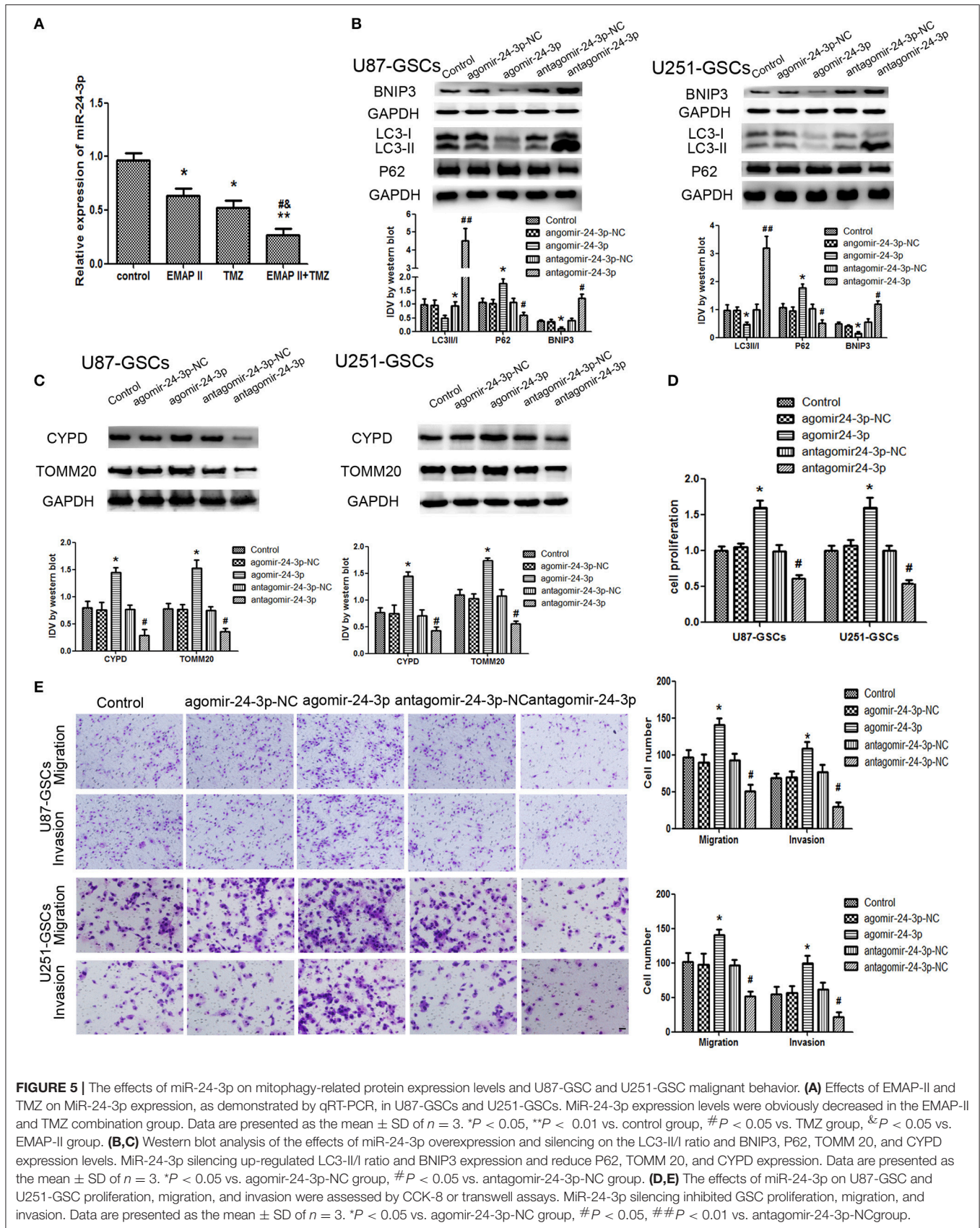
FIGURE 5 | The effects of miR-24-3p on mitophagy-related protein expression levels and U87-GSC and U251-GSC malignant behavior. **(A)** Effects of EMAP-II and TMZ on MiR-24-3p expression, as demonstrated by qRT-PCR, in U87-GSCs and U251-GSCs. MiR-24-3p expression levels were obviously decreased in the EMAP-II and TMZ combination group. Data are presented as the mean ± SD of $n = 3$. *$P < 0.05$, **$P < 0.01$ vs. control group, #$P < 0.05$ vs. TMZ group, &$P < 0.05$ vs. EMAP-II group. **(B,C)** Western blot analysis of the effects of miR-24-3p overexpression and silencing on the LC3-II/I ratio and BNIP3, P62, TOMM 20, and CYPD expression levels. MiR-24-3p silencing up-regulated LC3-II/I ratio and BNIP3 expression and reduce P62, TOMM 20, and CYPD expression. Data are presented as the mean ± SD of $n = 3$. *$P < 0.05$ vs. agomir-24-3p-NC group, #$P < 0.05$ vs. antagomir-24-3p-NC group. **(D,E)** The effects of miR-24-3p on U87-GSC and U251-GSC proliferation, migration, and invasion were assessed by CCK-8 or transwell assays. MiR-24-3p silencing inhibited GSC proliferation, migration, and invasion. Data are presented as the mean ± SD of $n = 3$. *$P < 0.05$ vs. agomir-24-3p-NC group, #$P < 0.05$, ##$P < 0.01$ vs. antagomir-24-3p-NCgroup.
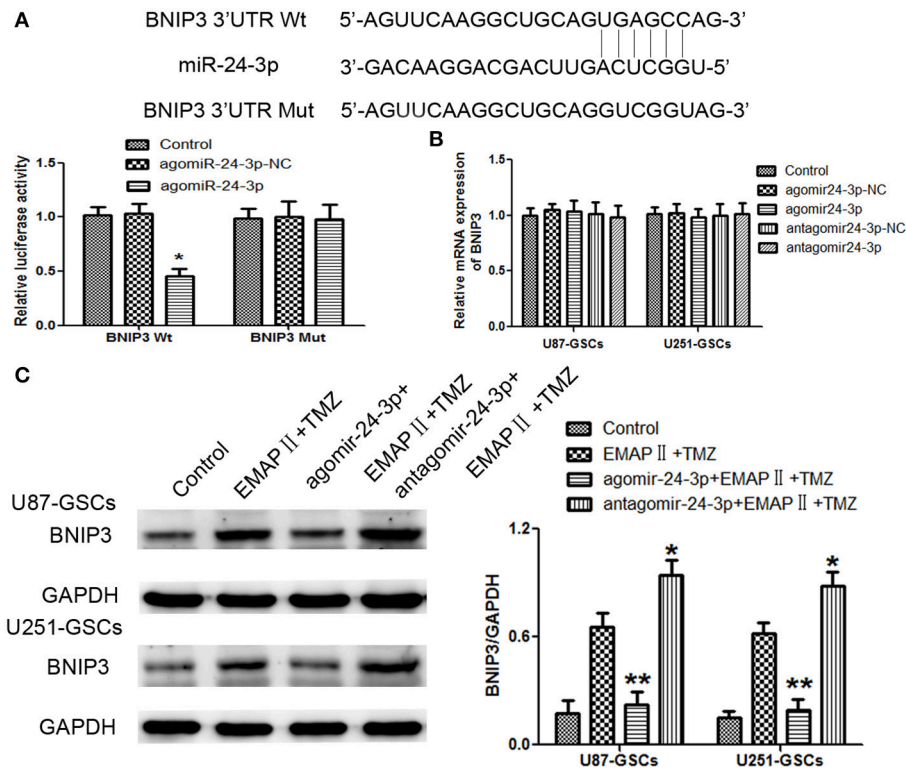
FIGURE 6 | BNIP3 was the direct target of miR-24-3p, and its expression level changed after miR-24-3p overexpression or silencing in U87-GSCs and U251-GSCs. **(A)** Relative luciferase activity was expressed as firefly/renilla luciferase activity. Luciferase activity was significantly decreased in the Wt BNIP3 3′ untranslated region (3′UTR)+agomir-24-3p group. Data are presented as the mean ± SD of $n = 3$. *$P < 0.05$ vs. agomir-24-3p-NC group. **(B)** BNIP3 relative mRNA expression levels were detected by qRT-PCR in U87-GSCs and U251-GSCs after miR-24-3p overexpression or silencing. MiR-24-3p overexpression or silencing do not influence BNIP3 mRNA expression. Data are presented as the mean ± SD of $n = 3$. **(C)** Western blot analysis of BNIP3 levels in U87-GSCs and U251-GSCs treated with EMAP-II and TMZ on the basis of miR-24-3p overexpression or silencing. Compared with EMAP-II+TMZ group, the expression of BNIP3 was reduced in agomir-24-3p+ EMAP-II+TMZ group. The opposite result was in antagomir-24-3p+EMAP-II+TMZ group. Data are presented as the mean ± SD of $n = 3$, **$P < 0.01$ vs. EMAP-II+TMZ group, *$P < 0.05$ vs. EMAP-II+TMZgroup.

was affected by TMZ in a time-dependent manner over 24, 48, and 72 h of treatment. In addition, we found that the suppressive effects of TMZ on GSCs were also dose-dependent. However, when the TMZ concentration was 400 μM or higher, this dose-dependent effect was no longer observed, a finding consistent with those of other studies. Yu et al. found that the cytotoxic effects of TMZ on U251-GSCs and U87-GSCs were time- and dose-dependent and that 200 μM TMZ treatment for 48 h could decrease cell viability by almost 30% (Yu et al., 2015). In recent years, studies have shown that EMAP-II plays an anti-tumor role through several processes, as the agent inhibits angiogenesis, promotes endothelial cell apoptosis and directly promotes tumor cell autophagy and apoptosis (Crippa et al., 2008; Li Z. et al., 2014; Ma et al., 2015; Chen et al., 2016). EMAP-II is still in the experimental study stage at present. Some studies have found that EMAP-II could facilitate TNF-R1 apoptotic signaling, which exerts anti-tumor functions (van Horssen et al., 2006). It also increases the permeability of blood-tumor barrier. Both are of benefit to killing tumor cells. Therefore, we think that EMAP-II has a good applied future in

the clinical practice. However, whether EMAP-II can enhance the cytotoxicity of TMZ remains unclear. It has been reported that low-dose EMAP-II generated cytotoxic effects through the PI3K/Akt/FoxO1 axis in U87-GSCs (Liu et al., 2014). TMZ could activate the Akt/glycogen synthase kinase-3ß pathway to induce glioma cell apoptosis via oncoprotein c-Myc (De Salvo et al., 2011) and exerted anti-tumor effects through the AKT-mTOR pathway in the GBM8901 glioma cell line (Chen et al., 2015). EMAP-II and TMZ affected glioma cells through a similar pathway, indicating that EMAP-II may strengthen the cytotoxic effects of TMZ. Our team have proved that the combination of EMAP-II and TMZ kill GSCs by inducing autophagy. Autophagy inhibitors weaken the cytotoxic effect of EMAP-II and TMZ on GSCs. Our research results are consistent with previous studies(Zhou et al., 2017). We also found that EMAP-II and TMZ kill GSCs through inducing mitophagy. We found that the cytotoxic effects of TMZ on GSCs were significantly enhanced and that GSC migration and invasion were also inhibited after EMAP-II pretreatment, but the concrete mechanisms underlying these effects remain to be investigated further.
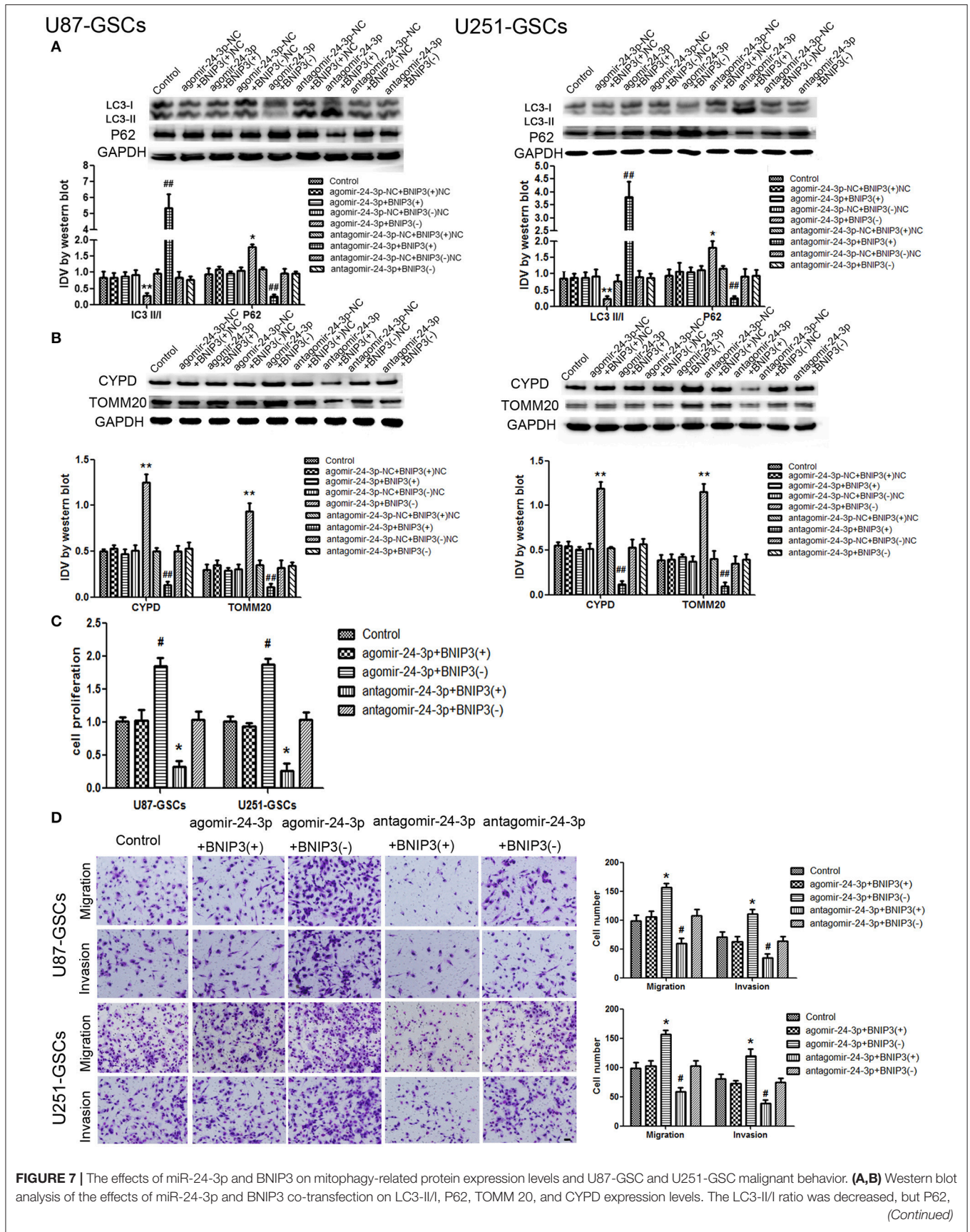
FIGURE 7 | The effects of miR-24-3p and BNIP3 on mitophagy-related protein expression levels and U87-GSC and U251-GSC malignant behavior. **(A,B)** Western blot analysis of the effects of miR-24-3p and BNIP3 co-transfection on LC3-II/I, P62, TOMM 20, and CYPD expression levels. The LC3-II/I ratio was decreased, but P62,

(Continued)

Mitophagy plays an important role in a variety of diseases, such as diabetes, cancer and degenerative diseases of the nervous system (Greene et al., 2003; Soleimanpour et al., 2015; Fader et al., 2016; Wilfinger et al., 2016). Consequently, mitophagy has been regarded as a target in anti-tumor therapy. Recently, some chemotherapy drugs were also found to exert anti-tumor effects by inducing mitophagy. For example, salinomycin promoted mitophagy to inhibit the growth of breast cancer and prostate cancer cells (Jangamreddy et al., 2013), and sodium selenite induced superoxide-mediated mitophagy and subsequent autophagic cell death in malignant glioma cells (Kim et al., 2007). EMAP-II can induce mitophagy in the U87, U118 and GSCs cell lines (Ma et al., 2015), but the specific mechanism underlying this effect remains unclear. TMZ has been found to induce mitochondrial-mediated autophagy and reduce the quantity of mitochondria in the U87 cell line (Lin et al., 2012). Our results showed the combination of EMAP-II and TMZ promoted the formation of autophagosome by transmission electron microscopy and increased the overlap between LC3 and Mito-Tracker or Lyso-Tracker by immunofluorescence staining. EMAP-II and TMZ up-regulated LC3II/I ratio and BNIP3 expression but down-regulated P62, TOMM20, and CYPD expression, indicating promoting mitophagy. These results indicated that the combination of EMAP-II and TMZ inhibited GSC malignant behavior by enhancing mitophagy.
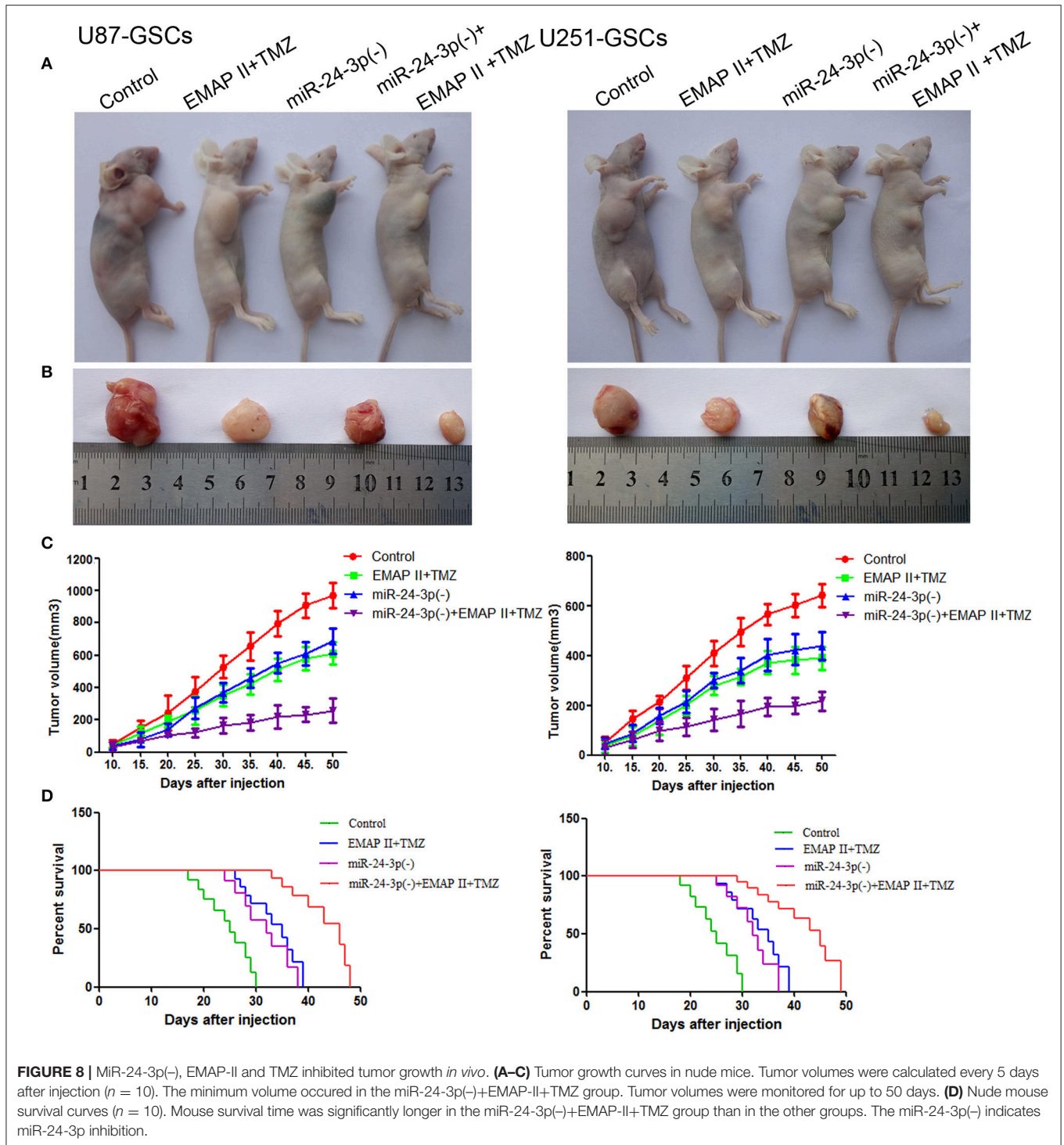
BNIP3 is distributed in the mitochondrial outer membrane and interacts with LC3 through the LC3-interacting region (LIR) to trigger excessive mitophagy (Hanna et al., 2012; Zhu et al., 2013). Arsenic trioxide and ceramide can upregulate BNIP3 expression to induce mitophagy in glioma (Daido et al., 2004; Kanzawa et al., 2005). We confirmed that the combination of EMAP-II and TMZ inhibited the biological behavior of GSCs by upregulated BNIP3 expression. BNIP3 overexpression enhanced the effect of EMAP-II and TMZ, which up-regulated the LC3II and down-regulated the expression level of P62, TOMM20 and CYPD, and inhibited the biological behavior of GSCs. BNIP3 knockdown exerted the opposite effect. The results of the above demonstrated the combination of EMAP-II and TMZ induced mitophagy by upregulating BNIP3 expression. BNIP3 overexpression could directly enhance the synergistic anti-tumor effects of EMAP-II and TMZ by inducing mitophagy. However, BNIP3 knockdown exerted the opposite effects. These results indicated that BNIP3-mediated mitophagy is one of the anti-tumor mechanisms underlying the effects of the combination of EMAP-II and TMZ. Abnormal increases in BNIP3 expression are affected by HIF-1 expression, which is positively correlated with tumor metastasis in non-small cell lung cancer (Giatromanolaki et al., 2004). BNIP3 silencing caused

by promoter methylation and histone acetylation is associated with chemotherapy resistance and worse survival, and BNIP3 restoration enhances chemosensitivity and promotes tumor cell apoptosis in gastric and colon cancer (Murai et al., 2005). These results indicates BNIP3 loss caused by various reasons is related with tumor progression, which consists with our results.

MiRNAs plays key roles in tumourigenesis and tumor progression as oncomirs (oncogenic miRNAs) or tumor suppressors. EMAP-II upregulated ATG7 and ATG5 to enhance U87 and U251 glioma cell autophagy via miR20a down-regulation (Chen et al., 2016). It has also been reported that TMZ upregulated ATG7 expression to induce autophagy by down-regulating miR-17 (Comincini et al., 2013). Previous study show miR-24-3p promoted cell proliferation and inhibited apoptosis in human breast cancer cells by targeting p27Kip1 (Lu et al., 2015). Moreover, miR-24-3p promoted cell proliferation in glioma cells via cooperative regulation of MXI1 (Xu et al., 2013). The results of these studies suggested that miR-24-3p may serve as an oncomir. And can EMAP-II and TMZ regulated mitophagy via miR-24-3p? Our results showed that the combination of EMAP-II and TMZ reduced miR-24-3p expression. MiR-24-3p overexpression decreased the LC3-II/I ratio and increased P62, TOMM20, and CYPD expression levels. MiR-24-3p overexpression also promoted the abilities of GSC proliferation, migration, and invasion. While miR-24-3p knockdown exerts the opposite effects. All the results indicated that combination treatment with EMAP-II and TMZ induced mitophagy and inhibited GSC malignant behavior by down-regulating miR-24-3p.

MiRNAs can bind to the 3′-UTRs of target mRNAs and block their translation. MiR-137 inhibited mitophagy by regulating the mitophagy receptors FUNDC1 and NIX (Li W. et al., 2014). BNIP3 was found to be the target gene of miR-24-3p using bioinformatics software. Dual-luciferase reporter assay illustrated that miR-24-3p binds with the 3′-UTR of BNIP3 mRNA. BNIP3 overexpression reversed the effects of agomir-24-3p on the LC3 II/I ratio and P62, TOMM 20, and CYPD expression, and BNIP3 knockdown reversed the effects of antagomir-24-3p on the LC3 II/I ratio and P62, TOMM 20, and CYPD expression. These resultsillustrate that miR-24-3p negatively regulates BNIP3, which inhibits mitophagy and promotes GSC proliferation, migration and invasion. Furthermore, we also found that combination of miR-24-3p(–), EMAP-II and TMZ inhibited tumor growth *in vivo*.

In summary, we have provided strong experimental evidence that EMAP-II can enhance the inhibitory effects of TMZ on GSC viability, migration and invasion. Regarding the mechanisms underlying this effect, the combination of TMZ and EMAP-II

FIGURE 8 | MiR-24-3p(–), EMAP-II and TMZ inhibited tumor growth *in vivo*. **(A–C)** Tumor growth curves in nude mice. Tumor volumes were calculated every 5 days after injection (*n* = 10). The minimum volume occured in the miR-24-3p(–)+EMAP-II+TMZ group. Tumor volumes were monitored for up to 50 days. **(D)** Nude mouse survival curves (*n* = 10). Mouse survival time was significantly longer in the miR-24-3p(–)+EMAP-II+TMZ group than in the other groups. The miR-24-3p(–) indicates miR-24-3p inhibition.

upregulated BNIP3 expression by down-regulating miR-24-3p, thereby strengthening BNIP3-mediated mitophagy. Because of its anti-tumor effects, the combination of EMAP-II and TMZ may represent a novel therapeutic strategy for treating glioma.

ETHICS STATEMENT

The animals were raised in accordance with the guidelines of the Laboratory Animal Centre of Shengjing Hospital.

AUTHOR CONTRIBUTIONS

LL and YX: Conceived and designed the study; JZ, LL, and YX: Developed the methodology and performed the *in vitro* and *in vivo* experiments; YM and YL: Reviewed and interpreted the data; ZheL and ZhiL: Analyzed the data and supervised the study; JZ: Wrote the manuscript. All authors read and approved the final manuscript.

ACKNOWLEDGMENTS

SUPPLEMENTARY MATERIAL

The Supplementary Material for this article can be found online at: https://www.frontiersin.org/articles/10.3389/fnmol.2018.00092/full#supplementary-material

Supplementary Figure 1 | Isolation and identification of GSCs. **(A)** GSCs-U87 and GSCs-U251 stained for Nestin (red) andCD133 (green) by immunofluorescence staining. **(B)** GSC-U87 and GSC-U251 spheres were differentiated and then stained for GFAP (red) and beta-tubulin III (green) by immunofluorescence staining.

Supplementary Figure 2 | Western blot analysis of the LC3-II/I ratio and BNIP3, P62, TOMM 20, and CYPD expression levels in U87-GSCs and U251-GSCs xenografted tumor. The LC3-II/I ratio and BNIP3 increased, but P62, TOMM 20, and CYPD expression decreased in the miR-24-3p(–)+EMAP-II+TMZ group. Data are presented as the mean ± SD of $n = 3$. $*P < 0.05$ vs. control group, $^{\#}P < 0.05$ vs. miR-24-3p(–) group, $^{\$}P < 0.05$ vs. EMAP-II+TMZ group. The miR-24-3p(–) indicates miR-24-3p inhibition.

REFERENCES

Auffinger, B., Tobias, A. L., Han, Y., Lee, G., Guo, D., Dey, M., et al. (2014). Conversion of differentiated cancer cells into cancer stem-like cells in a glioblastoma model after primary chemotherapy. *Cell Death Differ.* 21, 1119–1131. doi: 10.1038/cdd.2014.31

Awasthi, N., Zhang, C. H., Hinz, S., Schwarz, M. A., and Schwarz, R. E. (2013). Enhancing sorafenib-mediated sensitization to gemcitabine in experimental pancreatic cancer through EMAP II. *J. Exp. Clin. Cancer Res.* 32:12. doi: 10.1186/1756-9966-32-12

Bao, S., Wu, Q., Sathornsumetee, S., Hao, Y., Li, Z., Hjelmeland, A. B., et al. N. (2006). Stem cell-like glioma cells promote tumor angiogenesis through vascular endothelial growth factor. *Cancer Res.* 66, 7843–7848. doi: 10.1158/0008-5472.CAN-06-1010

Bellot, G., Garcia-Medina, R., Gounon, P., Chiche, J., Roux, D., Pouysségur, J., et al. (2009). Hypoxia-induced autophagy is mediated through hypoxia-inducible factor induction of BNIP3 and BNIP3L via their BH3 domains. *Mol. Cell. Biol.* 29, 2570–2581. doi: 10.1128/MCB.00166-09

Berger, A. C., Alexander, H. R., Tang, G., Wu, P. S., Hewitt, S. M., Turner, E., et al. (2000a). Endothelial monocyte activating polypeptide II induces endothelial cell apoptosis and may inhibit tumor angiogenesis. *Microvasc. Res.* 60, 70–80. doi: 10.1006/mvre.2000.2249

Berger, A. C., Tang, G., Alexander, H. R., and Libutti, S., K. (2000b). Endothelial monocyte-activating polypeptide II, a tumor-derived cytokine that plays an important role in inflammation, apoptosis, and angiogenesis. *J. Immunother.* 23, 519–527. doi: 10.1097/00002371-200009000-00002

Chen, J., Liu, L., Liu, Y., Liu, X., Qu, C., Meng, F., et al. (2016). Low-dose endothelial-monocyte-activating polypeptide-II induced autophagy by down-regulating miR-20a in U-87 and U-251 glioma cells. *Front. Cell. Neurosci.* 10:128. doi: 10.3389/fncel.2016.00128

Chen, C. M., Syu, J. P., Way, T. D., Huang, L. J., Kuo, S. C., Lin, C. T., et al. (2015). BC3EE2,9B, a synthetic carbazole derivative, upregulates autophagy and synergistically sensitizes human GBM8901 glioblastoma cells to temozolomide. *Int. J. Mol. Med.* 36, 1244–1252. doi: 10.3892/ijmm.2015.2332

Comincini, S., Allavena, G., Palumbo, S., Morini, M., Durando, F., Angeletti, F., et al. (2013). microRNA-17 regulates the expression of ATG7 and modulates the autophagy process, improving the sensitivity to temozolomide and low-dose ionizing radiation treatments in human glioblastoma cells. *Cancer Biol. Ther.* 14, 574–586. doi: 10.4161/cbt.24597

Crippa, L., Gasparri, A., Sacchi, A., Ferrero, E., Curnis, F., and Corti, A. (2008). Synergistic damage of tumor vessels with ultra low-dose endothelial-monocyte activating polypeptide-II and neovasculature-targeted tumor necrosis factor-α. *Cancer Res.* 68, 1154–1161. doi: 10.1158/0008-5472.CAN-07-2085

Daido, S., Kanzawa, T., Yamamoto, A., Takeuchi, H., Kondo, Y., and Kondo, S. (2004). Pivotal role of the cell death factor BNIP3 in ceramide-induced autophagic cell death in malignant glioma cells. *Cancer Res.* 64, 4286–4293. doi: 10.1158/0008-5472.CAN-03-3084

De Salvo, M., Maresca, G., D'Agnano, I., Marchese, R., Stigliano, A., Gagliassi, R., et al. (2011). Temozolomide induced c-Myc-mediated apoptosis via Akt signalling in MGMT expressing glioblastoma cells. *Int. J. Radiat. Biol.* 87, 518–533. doi: 10.3109/09553002.2011.556173

Devin, A., and Rigoulet, M. (2007). Mechanisms of mitochondrial response to variations in energy demand in eukaryotic cells. *Am. J. Physiol. Cell Physiol.* 292, C52–C58. doi: 10.1152/ajpcell.00208.2006

Fader, C. M., Salassa, B. N., Grosso, R. A., Vergara, A. N., and Colombo, M. I. (2016). Hemin induces mitophagy in a leukemic erythroblast cell line. *Biol. Cell* 108, 77–95. doi: 10.1111/boc.201500058

Giatromanolaki, A., Koukourakis, M. I., Sowter, H. M., Sivridis, E., Gibson, S., Gatter, K. C., et al. (2004). BNIP3 expression is linked with hypoxia-regulated protein expression and with poor prognosis in non-small cell lung cancer. *Clin. Cancer Res.* 10, 5566–5571. doi: 10.1158/1078-0432.CCR-04-0076

Greene, J. C., Whitworth, A. J., Kuo, I., Andrews, L. A., Feany, M. B., and Pallanck, L. J. (2003). Mitochondrial pathology and apoptotic muscle degeneration in Drosophila parkin mutants. *Proc. Natl. Acad. Sci. U.S.A.* 100, 4078–4083. doi: 10.1073/pnas.0737556100

Hanna, R. A., Quinsay, M. N., Orogo, A. M., Giang, K., Rikka, S., and Gustafsson, A. B. (2012). Microtubule-associated protein 1 light chain 3 (LC3) interacts with Bnip3 protein to selectively remove endoplasmic reticulum and mitochondria via autophagy. *J. Biol. Chem.* 287, 19094–19104. doi: 10.1074/jbc.M111.322933

Jangamreddy, J. R., Ghavami, S., Grabarek, J., Kratz, G., Wiechec, E., Fredriksson, B. A., et al. J. (2013). Salinomycin induces activation of autophagy, mitophagy and affects mitochondrial polarity: differences between primary and cancer cells. *Biochim. Biophys. Acta* 1833, 2057–2069. doi: 10.1016/j.bbamcr.2013.04.011

Kanki, T., and Klionsky, D., J. (2009). Mitochondrial abnormalities drive cell death in Wolfram syndrome 2. *Cell Res.* 19, 922–923. doi: 10.1038/cr.2009.94

Kanki, T., Wang, K., Cao, Y., Baba, M., and Klionsky, D. J. (2009). Atg32 is a mitochondrial protein that confers selectivity during mitophagy. *Dev. Cell* 17, 98–109. doi: 10.1016/j.devcel.2009.06.014

Kanzawa, T., Germano, I. M., Komata, T., Ito, H., Kondo, Y., and Kondo, S. (2004). Role of autophagy in temozolomide-induced cytotoxicity for malignant glioma cells. *Cell Death Differ.* 11, 448–457. doi: 10.1038/sj.cdd.4401359

Kanzawa, T., Zhang, L., Xiao, L., Germano, I. M., Kondo, Y., and Kondo, S. (2005). Arsenic trioxide induces autophagic cell death in malignant glioma cells by upregulation of mitochondrial cell death protein BNIP3. *Oncogene* 24, 980–991. doi: 10.1038/sj.onc.1208095

Kim, E. H., Sohn, S., Kwon, H. J., Kim, S. U., Kim, M. J., Lee, S. J., et al. (2007). Sodium selenite induces superoxide-mediated mitochondrial damage and subsequent autophagic cell death in malignant glioma cells. *Cancer Res.* 67, 6314–6324. doi: 10.1158/0008-5472.CAN-06-4217

Kim, J., Fiesel, F. C., Belmonte, K. C., Hudec, R., Wang, W. X., Kim, C., et al. (2016). miR-27a and miR-27b regulate autophagic clearance of damaged mitochondria by targeting PTEN-induced putative kinase 1 (PINK1). *Mol. Neurodegener.* 11:55. doi: 10.1186/s13024-016-0121-4

Kurihara, Y., Kanki, T., Aoki, Y., Hirota, Y., Saigusa, T., Uchiumi, T., et al. (2012). Mitophagy plays an essential role in reducing mitochondrial production of reactive oxygen species and mutation of mitochondrial DNA by maintaining mitochondrial quantity and quality in yeast. *J. Biol. Chem.* 287, 3265–3272. doi: 10.1074/jbc.M111.280156

Li, Z., Liu, Y. H., Xue, Y. X., Liu, L. B., and Wang, P. (2014). Low-dose endothelial monocyte-activating polypeptide-ii increases permeability of blood-tumor barrier by caveolae-mediated transcellular pathway. *J. Mol. Neurosci.* 52, 313–322. doi: 10.1007/s12031-013-0148-8

Li, W., Zhang, X., Zhuang, H., Chen, H. G., Chen, Y. Q., Tian, W. L., et al. (2014). MicroRNA-137 is a novel Hypoxia-responsive MicroRNA that inhibits mitophagy via regulation of two mitophagy receptors FUNDC1 and NIX. *J.Biol. Chem.* 289, 10691–10701. doi: 10.1074/jbc.M113.537050

Li, Q. Q., Zhang, L., Wan, H. Y., Liu, M., Li, X., and Tang, H. (2015). CREB1-driven expression of miR-320a promotes mitophagy by down-regulating VDAC1 expression during serum starvation in cervical cancer cells. *Oncotarget* 6, 34924–34940. doi: 10.18632/oncotarget.5318

Lin, C. J., Lee, C. C., Shih, Y. L., Lin, C. H., Wang, S. H., Chen, T. H., et al. (2012). Inhibition of mitochondria- and endoplasmic reticulum stress-mediated autophagy augments temozolomide-induced apoptosis in glioma cells. *PLoS ONE* 7:e38706. doi: 10.1371/journal.pone.0038706

Lin, S. C., Liu, C. J., Lin, J. A., Chiang, W. F., Hung, P. S., and Chang, K. W. (2010). miR-24 up-regulation in oral carcinoma: positive association from clinical and *in vitro* analysis. *Oral Oncol.* 46, 204–208. doi: 10.1016/j.oraloncology.2009.12.005

Liu, J., Liu, L., Xue, Y., Meng, F., Li, S., Wang, P., et al. (2014). Anti-neoplastic activity of low-dose endothelial-monocyte activating polypeptide-II results from defective autophagy and G2/M arrest mediated by PI3K/Akt/FoxO1 axis in human glioblastoma stem cells. *Biochem. Pharmacol.* 89, 477–489. doi: 10.1016/j.bcp.2014.04.014

Louis, D. N., Perry, A., Reifenberger, G., von Deimling, A., Figarella-Branger, D., Cavenee, W. K., et al. (2016). The 2016 World Health Organization Classification of Tumors of the central nervous system: a summary. *Acta Neuropathol.* 131, 803–820. doi: 10.1007/s00401-016-1545-1

Lu, K., Wang, J., Song, Y., Zhao, S., Liu, H., Tang, D. B., et al. (2015). miRNA-24-3p promotes cell proliferation and inhibits apoptosis in human breast cancer by targeting p27Kip1. *Oncol. Rep.* 34, 995–1002. doi: 10.3892/or.2015.4025

Ma, J., Meng, F., Li, S., Liu, L., Zhao, L., Liu, Y., et al. (2015). Autophagy induction by endothelial-monocyte activating polypeptide II contributes to the inhibition of malignant biological behaviors by the combination of EMAP II with rapamycin in human glioblastoma. *Front. Mol. Neurosci.* 8:74. doi: 10.3389/fnmol.2015.00074

Murai, M., Toyota, M., Suzuki, H., Satoh, A., Sasaki, Y., Akino, K., et al. (2005). Aberrant methylation and silencing of the BNIP3 gene in colorectal and gastric cancer. *Clin. Cancer Res.* 11, 1021–1027.

Nabors, L. B. (2016). Central nervous system: notable developments in the management of primary and recurrent gliomas. *J. Natl. Compr. Canc. Netw.* 14, 681–684. doi: 10.6004/jnccn.2016.0192

Ohka, F., Natsume, A., and Wakabayashi, T. (2012). Current trends in targeted therapies for glioblastoma multiforme. *Neurol. Res. Int.* 2012:878425. doi: 10.1155/2012/878425

Ostrom, Q. T., Gittleman, H., Fulop, J., Liu, M., Blanda, R., Kromer, C., et al. (2015). CBTRUS statistical report: primary brain and central nervous system tumors diagnosed in the United States in 2008-2012. *Neuro Oncol,* 17(Suppl. 4), iv1–iv62. doi: 10.1093/neuonc/nov189

Pace, A., Vidiri, A., Galiè, E., Carosi, M., Telera, S., Cianciulli, A. M., et al. (2003). Temozolomide chemotherapy for progressive low-grade glioma: clinical benefits and radiological response. *Ann. Oncol.* 14, 1722–1726. doi: 10.1093/annonc/mdg502

Rapp, M., Sadat, H., Slotty, P. J., Steiger, H. J., Budach, W., and Sabel, M. (2015). Feasibility of the EORTC/NCIC trial protocol in a neurosurgical outpatient unit: the case for neurosurgical Neuro-Oncology. *J. Neurol. Surg. A Cent. Eur. Neurosurg.* 76, 298–302. doi: 10.1055/s-0034-1396437

Singh, S. K., Hawkins, C., Clarke, I. D., Squire, J. A., Bayani, J., Hide, T., et al. (2004). Identification of human brain tumour initiating cells. *Nature* 432, 396–401. doi: 10.1038/nature03128

Soleimanpour, S. A., Ferrari, A. M., Raum, J. C., Groff, D. N., Yang, J. X., Kaufman, B. A., et al. (2015). Diabetes susceptibility genes Pdx1 and Clec16a function in a pathway regulating mitophagy in β-cells. *Diabetes* 64, 3475–3484. doi: 10.2337/db15-0376

Stupp, R., Mason, W. P., van den Bent, M. J., Weller, M., Fisher, B., Taphoorn, M. J., et al. (2005). Radiotherapy plus concomitant and adjuvant temozolomide for glioblastoma. *N. Engl. J. Med.* 352, 987–996. doi: 10.1056/NEJMoa043330

Tolkovsky, A. M., Xue, L., Fletcher, G. C., and Borutaite, V. (2002). Mitochondrial disappearance from cells: a clue to the role of autophagy in programmed cell death and disease? *Biochimie* 84, 233–240. doi: 10.1016/S0300-9084(02) 01371-8

Tu, Y., Gao, X., Li, G., Fu, H., Cui, D., Liu, H., et al. (2013). MicroRNA-218 inhibits glioma invasion, migration, proliferation, and cancer stem-like cell self-renewal by targeting the polycomb group gene Bmi1. *Cancer Res.* 73, 6046–6055. doi: 10.1158/0008-5472.CAN-13-0358

van Horssen, R., Rens, J. A., Schipper, D., Eggermont, A. M., and ten Hagen, T. L. (2006). EMAP-II facilitates TNF-R1 apoptotic signalling in endothelial cells and induces TRADD mobilization. *Apoptosis* 11, 2137–2145. doi: 10.1007/s10495-006-0284-5

Wilfinger, N., Austin, S., Scheiber-Mojdehkar, B., Berger, W., Reipert, S., Praschberger, M., et al. (2016). Novel p53-dependent anticancer strategy by targeting iron signaling and BNIP3L-induced mitophagy. *Oncotarget* 7, 1242–1261. doi: 10.18632/oncotarget.6233

Xu, W., Liu, M., Peng, X., Zhou, P., Zhou, J., Xu, K., et al. (2013). miR-24-3p and miR-27a-3p promote cell proliferation in glioma cells via cooperative regulation of MXI1. *Int. J. Oncol.* 42, 757–766. doi: 10.3892/ijo. 2012.1742

Yu, Z., Zhao, G., Xie, G., Zhao, L., Chen, Y., Yu, H., et al. (2015). Metformin and temozolomide act synergistically to inhibit growth of glioma cells and glioma stem cells *in vitro* and *in vivo*. *Oncotarget* 6, 32930–32943. doi: 10.18632/oncotarget.5405

Zhang, F. L., Wang, P., Liu, Y. H., Liu, L. B., Liu, X. B., Li, Z., et al. (2013). Topoisomerase I inhibitors, shikonin and topotecan, inhibit growth and induce apoptosis of glioma cells and glioma stem cells. *PLoS ONE* 8:e81815. doi: 10.1371/journal.pone.0081815

Zhang, H., Bosch-Marce, M., Shimoda, L. A., Tan, Y. S., Baek, J. H., Wesley, J. B., et al. (2008). Mitochondrial autophagy is an HIF-1-dependent adaptive metabolic response to hypoxia. *J. Biol. Chem.* 283, 10892–10903. doi: 10.1074/jbc.M800102200

Zhou, W., Liu, L., Xue, Y., Zheng, J., Liu, X., Ma, J., et al. (2017). Combination of endothelial-monocyte-activating polypeptide-II with temozolomide suppress malignant biological behaviors of human glioblastoma stem cells via miR-590-3p/MACC1 Inhibiting PI3K/AKT/mTOR signal pathway. *Front. Mol. Neurosci.* 10:68. doi: 10.3389/fnmol.2017.00068

Zhu, Y., Massen, S., Terenzio, M., Lang, V., Chen-Lindner, S., Eils, R., et al. (2013). Modulation of serines 17 and 24 in the LC3-interacting region of Bnip3 determines pro-survival mitophagy versus apoptosis. *J. Biol. Chem.* 288, 1099–1113. doi: 10.1074/jbc.M112.399345